JOURNAL OF MATERIALS SCIENCE 26 (1991) 5374–5382

Damage zone development in PVC under a multiaxial tensile stress state

A. TSE, E. SHIN, A. HILTNER, E. BAER
Department of Macromolecular Science, and Center for Applied Polymer Research, Case Western Reserve University, Cleveland, OH 44106, USA

The irreversible deformation mechanisms of poly(vinyl chloride) with a semicircular notch under slow tensile loading have been studied as a function of sheet thickness. Initially, core yielding was observed in the optical microscope as two families of slip lines growing from the notch surface in the centre of the specimen. The size and shape of the core yielding zone could be described by plasticity analysis. A stress-whitened zone subsequently initiated near the tip of the slip line zone. The stress whitening was caused by 1 μm voids that were visible in the scanning electron microscope. The mean stress for stress whitening was calculated to be 43.0 ± 1.5 MPa by a plastic stress analysis of a pressure-dependent yield material. By assuming a constant mean stress along the boundary of the stress-whitened zone, the one-dimensional shift of the elastic stress distribution was obtained. At higher stresses, hinge shear and intersecting shear were observed for thick and thin sheet, respectively.

1. Introduction

Crazing, shear banding and stress whitening have all been observed in rigid poly(vinyl chloride) (PVC) formulated without plasticizers or rubber modification [1, 2]. Unnotched PVC sheet deformed in tension typically shows crazing prior to necking [3, 4]. In this type of test, crazes form first and when necking occurs they pass almost unaltered through the neck. Interaction of crazes with plastic deformation modes is more readily apparent in tests where a significant degree of triaxiality is present. With a sharp notch, a multiple craze zone is observed at the crack tip [5, 6]. Although in this case multiple crazing was thought to be the primary source of fracture toughness, the coexistence of a yield zone which follows the Dugdale model has been suggested [7, 8].

The circular or semicircular notch is particularly attractive when the objective is to examine the damage zone in a triaxial stress state while minimizing the tendency for crack growth. This geometry has been used to clarify the shear yielding modes in polycarbonate and subsequently to analyse the thickness dependence in terms of plasticity concepts [9]. Stress states with a significant degree of triaxiality are required if the role of dilational mechanisms is to be measured directly. The elastic stress distribution at a semicircular notch was used to determine the mean stress condition for cavitation in impact-modified PVC [10]. The corresponding volume strain was the same for various impact modifiers, and because the volume strain was also independent of temperature and blend composition, was thought to be the controlling parameter for cavitation in PVC blends.

Tests utilizing blunt notch geometries clearly show a yielded zone in PVC at the notch tip. A slip line zone emanating from the notch tip similar to that observed in polycarbonate has been described [11]. A disc-like craze subsequently nucleated at the tip of the plastic zone [12, 13]. Because crazing requires void formation, the dilational stress at the elastic–plastic boundary was thought to be responsible for craze and fracture initiation [14], although if the sheet is thin enough, the condition for general yielding may be achieved before craze-initiated fracture [15]. Formation of a diffuse stress-whitened zone near the elastic–plastic boundary, instead of crazing, has also been described [13]. Scattering of visible light from microvoids about 1 μm in size causes the stress whitening [16]. The inhomogeneities that act as stress raisers to promote the profuse microvoiding may be particles of insoluble additives [1, 2]. In this study, the development of the damage zone at a semicircular notch in PVC sheet was examined. In this instance, crazing and stress-whitening mechanisms were encountered in addition to shear yielding modes, and comparisons were made with other materials including polycarbonate, which deforms by shear yielding, and impact-modified PVC where cavitation is the primary mechanism.

2. Experimental procedure

A low molecular weight poly(vinyl chloride) (PVC) (Georgia Gulf 2066, $K = 55$) with 2.5 p.h.r. heat stabilizer (Mark 1900), 1.5 p.h.r. processing aid (Paraloid K-175), 1.5 p.h.r internal lubricant (Loxiol HOB 7111) and 0.3 p.h.r. ultraviolet stabilizer (Tinuvin 328), was supplied by The Dow Chemical Company in the form of roll-milled blankets that had been prepared as described previously [10]. Sheets were moulded to

0022–2461/91 $03.00 + .12

three thicknesses, 1.6, 3.6 and 4.9 mm, using the same conditions as previously [10]. A 1 mm radius semicircular notch was machined midway along one edge of 152 mm × 20 mm rectangular specimens which were then annealed at 80 °C for 4 h. When cartesian coordinates were used, the x, y and z directions were identified with the specimen width, length and thickness, respectively, with the origin at the notch centre.

The notched specimens were mounted in an Instron machine with 100 mm separating the grips. Tensile tests were performed at ambient temperature with a crosshead speed of 0.1 mm min^{-1}; the damage zone at the notch was photographed during loading with a travelling microscope in the transmission mode at a magnification of X20.

Unnotched ASTM D638 Type I specimens were loaded to failure at several crosshead speeds between 0.1 and 10 mm min^{-1} in order to determine the rate dependence of the tensile yield stress. The crosshead speed of 10 mm min^{-1} was chosen to approximate the strain rate at the notch root for the testing conditions used to observe the damage zone [17], and the tensile yield stress determined at this crosshead speed was used in the analysis.

Some specimens were loaded to a specific position on the stress–displacement curve, removed from the Instron and sectioned in the yz plane. After a rough cut, these specimens were polished with silicon carbide paper and then with a suspension of aluminum powder down to 0.1 μm. The sections were viewed in an Olympus Model BH3 optical microscope in both the transmission and cross-polarized modes. Other specimens were unloaded, immersed in liquid nitrogen and deformed so that they fractured in a brittle manner in the xz plane through the pre-existing damage zone. The fracture surfaces were coated with about 5 nm carbon and examined in the Jeol 840A scanning electron microscope (SEM) at 5 kV. Both surfaces were examined to confirm that fracture had propagated through the damage zone.

3. Results and discussion

3.1. Damage zone

The stress–displacement curve of PVC with a semicircular notch is shown in Fig. 1 for the 3.6 mm thick sheet. The specimen was photographed during deformation, and the arrows indicate the positions at which the following sequence of micrographs was taken. At position 1 on the stress–displacement curve (32.5 MPa, Fig. 2a), core yielding was observed with the focus at the centre of the specimen as two families of flow lines growing out from the notch. The core yielding zone increased in size at position 2 (34.8 MPa, Fig. 2b) as the curving slip lines lengthened and more initiated from the notch surface. The average angle of intersection between the alpha and beta slip lines was 85° ± 2°. In addition to the slip lines, a stress-whitened zone was barely discernable at position 1 but was clear at position 2 as a dark region near the tip of the slip line zone. Both the stress-whitened zone and the core yielding zone continued to increase in size as the stress increased at position 3 (37.5 MPa, Fig. 2c). The tip of the slip line zone was obscured at position 4 (41.1 MPa, Fig. 2d) by the optical opacity of the stress-whitened zone.

3.2. Core yielding zone

Core yielding occurred at the notch root in the centre of the specimen where the triaxial stress constraint was a maximum. The plane strain core yielding at a semicircular notch of a non-work hardening perfectly plastic material has been described by logarithmic spirals [18]. The characteristic slip line field of the

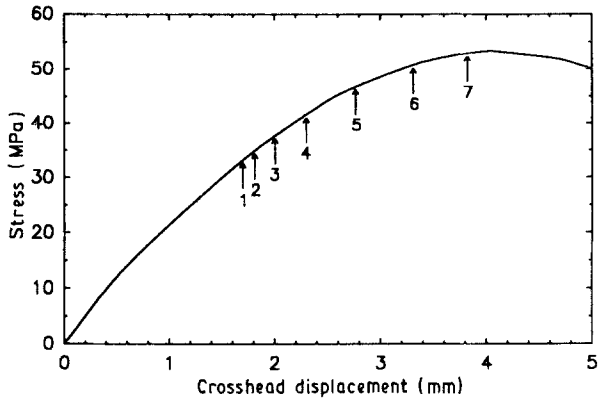

Figure 1 Stress–displacement curve of 3.6 mm thick PVC with a semicircular notch.

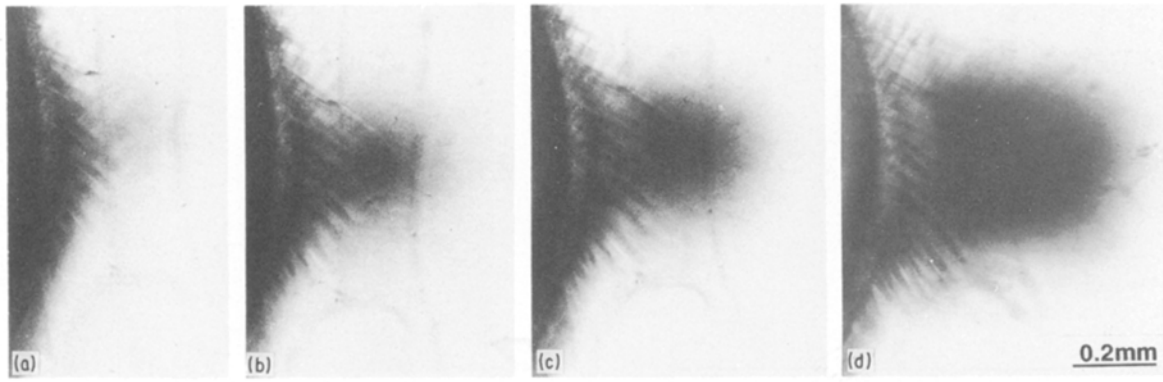

Figure 2 Optical micrographs of the damage zone of 3.6 mm thick PVC. (a) Position 1, 32.5 MPa, (b) position 2, 34.8 MPa, (c) position 3, 37.5 MPa, and (d) position 4, 41.1 MPa.

double logarithmic spirals is given by

$$\theta = \pm \ln(r/a) + \text{constant} \quad (1)$$

in polar coordinates (r, θ) where a is the notch radius. The signs indicate the two families of orthogonal alpha and beta slip lines that follow the directions of maximum shear stress.

Equation 1 predicts an angle of 90° between the alpha and beta slip lines based on a pressure-independent yield criterion. In general, glassy polymers are found to obey a pressure-dependent yield criterion where the yield stress increases with hydrostatic pressure. A widely used approach is the modified von Mises yield criterion with the form

$$k = k_0 - \mu\sigma_m \quad (2)$$

where k is the shear yield stress in pure shear, σ_m is the hydrostatic mean stress, and k_0 and μ are material parameters. A modification of Equation 1 for a pressure-dependent yield material has been proposed [12]

$$\theta \cot \psi = \pm \ln(r/a) + \text{constant} \quad (3)$$

where 2ψ is the angle between slip lines and is related to the pressure-dependency through $\mu = \cos 2\psi$ [12]. Using the published value of $\mu = 0.11$ for PVC [19, 20], the angle between alpha and beta slip lines was calculated to be 83.6° in good agreement with the observed value of 85° ± 2°.

3.3. Morphology of the stress-whitened zone

Contours of the stress-whitened zone at various stresses (cf. Fig. 2) showed how it changed in size and shape, Fig. 3. As the stress increased, the zone grew in only three directions in the xy plane, the near-notch boundary on the x-axis remained fixed at 0.12 mm from the notch surface.

A cross-section through the 3.6 mm thick specimen is shown in Fig. 4. The specimen was loaded to position 3 on the stress–displacement curve (cf. Fig. 2c) and sectioned in the yz plane through the stress-whitened zone. In the optical micrograph, the rectangular stress-whitened zone measured about 0.25 mm high and extended through the thickness except for a region at the edge. The region through the thickness that showed stress whitening was previously identified as the region of plane strain, while the region at the edge that was not stress whitened corresponded to a boundary layer of rapidly decreasing σ_{zz} [10]. It was consistent with previous observations on stress whitening of PVC blends that formation of the stress-whitened zone in PVC would also require a triaxial stress condition [10].

A specimen that had been loaded to a stress near position 5 in Fig. 1 was cryogenically fractured through the damage zone. A low-magnification scanning electron micrograph of the fracture surface created by brittle fracture through the pre-existing damage zone, Fig. 5a, showed the curved core yielding zone at the notch root. At higher magnification, Fig. 5b, the core yielding zone appeared as two families of ridges that intersected at an angle of approximately 90°. In the centre, the core yielding zone extended away from the notch about 0.1 mm, a distance that coincided with the near-notch boundary of the stress-whitened zone in side views of the damage zone. The region on the fracture surface further from the notch and adjacent to the core yielding zone that corresponded to the stress-whitened zone showed profuse cavitation when viewed at high magnification. Light scattering from these 1 μm voids would have made the voided region visible in the optical microscope as the stress-whitened zone. Comparison of high-magnification views of the core yielding zone, Fig. 5c, the stress-whitened zone, Fig. 5d, and the region beyond the stress-whitened zone, Fig. 5e, clearly showed that only the stress-whitened zone was voided. Previous reports of voiding in PVC suggested that additives in the PVC formulation acted as a second phase to promote cavitation [1, 2].

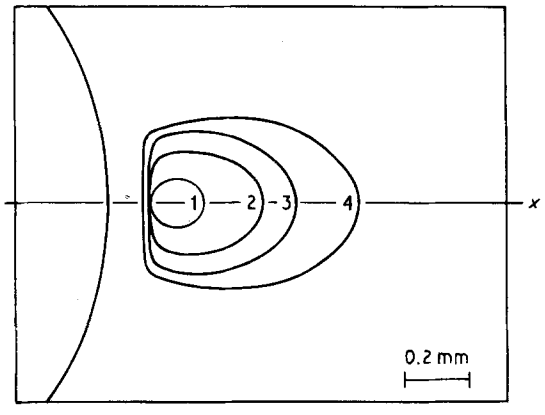

Figure 3 Contours of the stress-whitened zone at positions 1–4 on the stress–displacement curve for 3.6 mm thick PVC.

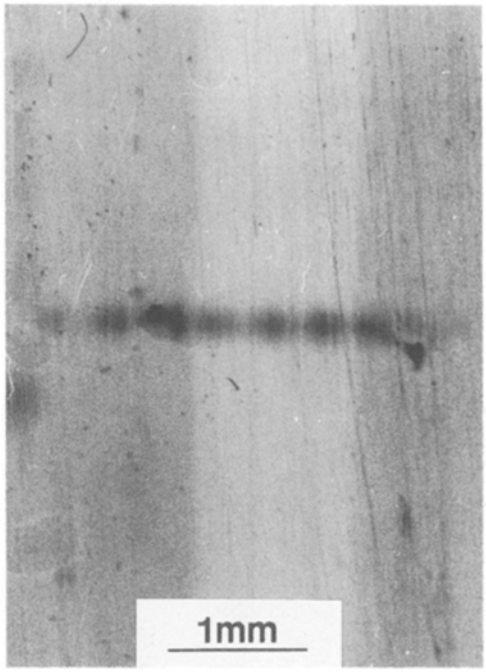

Figure 4 Cross-section of 3.6 mm thick PVC loaded to position 3 and sectioned in the yz direction through the stress-whitened zone.

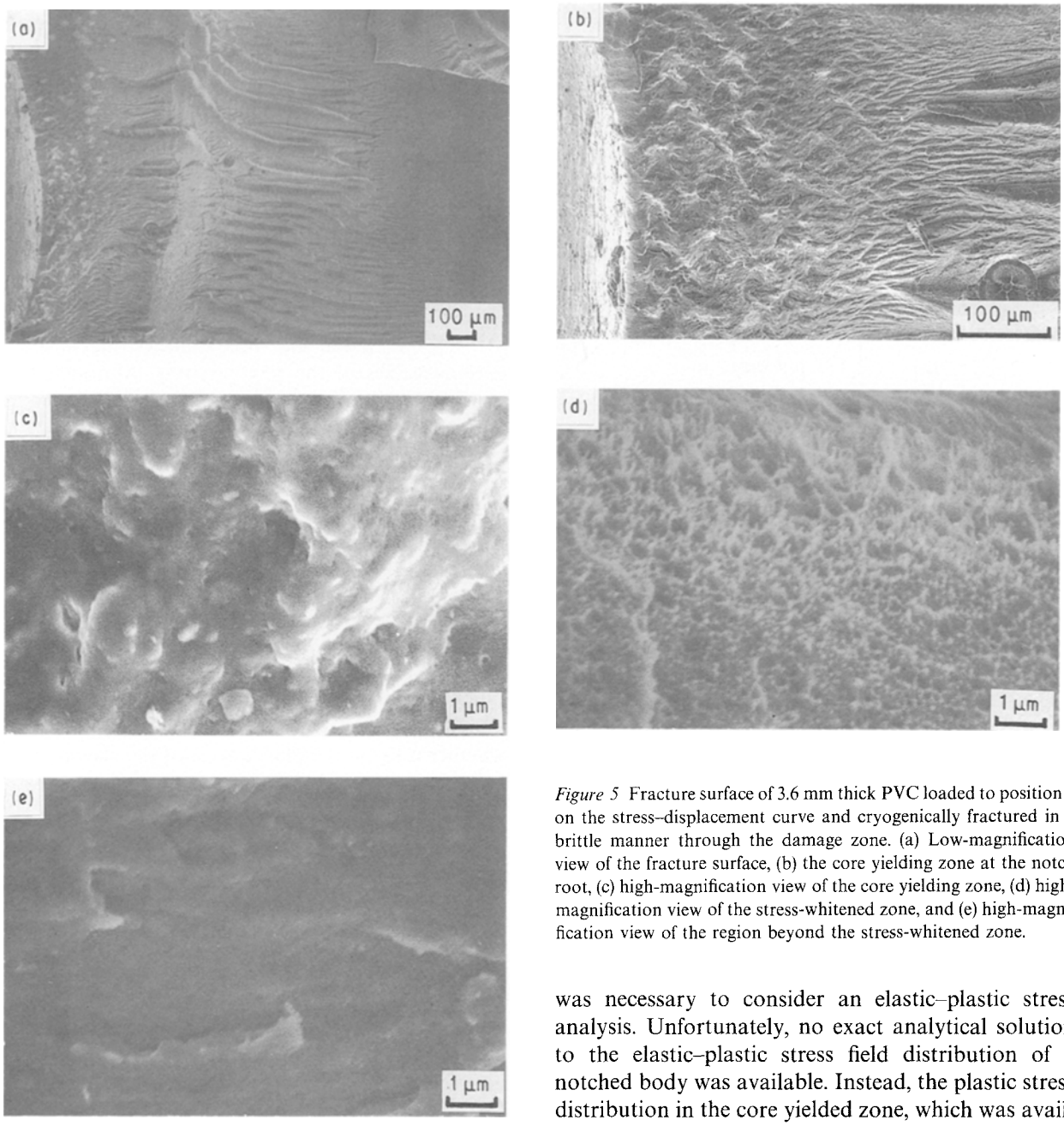

Figure 5 Fracture surface of 3.6 mm thick PVC loaded to position 5 on the stress–displacement curve and cryogenically fractured in a brittle manner through the damage zone. (a) Low-magnification view of the fracture surface, (b) the core yielding zone at the notch root, (c) high-magnification view of the core yielding zone, (d) high-magnification view of the stress-whitened zone, and (e) high-magnification view of the region beyond the stress-whitened zone.

3.4. Analysis of the stress-whitened zone

It was assumed that the previously established condition for stress whitening of PVC blends also applied to PVC, and the stress-whitened zone in PVC was controlled by a dilational mean stress condition. In the previous case, it was sufficient to use the plane strain elastic stress distribution at the notch in order to determine the mean stress from the boundary of the stress-whitened zone. However, the shape of the stress-whitened zone in PVC was very different from the crescent-shaped zone emanating from the notch root that fits the elastic mean stress condition. Furthermore, unlike the blends, stress whitening of PVC was preceded by core yielding at the notch root. The stress-whitened zone was seen as being superimposed on an elastic–plastic interface so that the near-notch boundary lay within the plastic yielded zone and the far-notch boundary in the surrounding elastic region. Because the presence of a plastic yielded zone at the notch root altered the stress distribution, it was necessary to consider an elastic–plastic stress analysis. Unfortunately, no exact analytical solution to the elastic–plastic stress field distribution of a notched body was available. Instead, the plastic stress distribution in the core yielded zone, which was available in the literature, was used to obtain the plastic mean stress condition for stress whitening from the near-notch boundary of the stress-whitened zone.

The plastic stress distribution along the x-axis in the slip line field of a perfectly plastic material for the case of a semicircular notch is given by [18]

$$\sigma_{rr} = 2k_o[\ln(r/a)] \quad (4)$$

$$\sigma_{\theta\theta} = 2k_o[1 + \ln(r/a)] \quad (5)$$

$$\sigma_{r\theta} = 0 \quad (6)$$

where σ_{rr} and $\sigma_{\theta\theta}$ are the normal stresses and $\sigma_{r\theta}$ is the shear stress. The mean stress in the plastic zone for plane strain conditions with $\nu = 0.5$ is then given by

$$\sigma_m = (\sigma_{rr} + \sigma_{\theta\theta} + \sigma_{zz})/3$$

$$= k_o[1 + 2\ln(r/a)] \quad (7)$$

One result of Equation 7 is that the mean stress increased with distance away from the notch root.

It has been noted that Equations 4–6 tend to overestimate the stress components around the notch because, in general, the yield criterion of polymers is

pressure dependent. Alternatively, the plastic stress distribution for a pressure-dependent material is given by [11, 12]

$$\sigma_{rr} = \frac{k_o}{\mu}\left[1 - \left(\frac{r}{a}\right)^{-2\mu/(1+\mu)}\right] \quad (8)$$

$$\sigma_{\theta\theta} = \frac{k_o}{\mu}\left[1 - \left(\frac{1-\mu}{1+\mu}\right)\left(\frac{r}{a}\right)^{-2\mu/(1+\mu)}\right] \quad (9)$$

$$\sigma_{r\theta} = 0 \quad (10)$$

The corresponding mean stress, σ_m, is given by

$$\sigma_m = \frac{k_o}{\mu}\left[1 - \left(\frac{1}{1+\mu}\right)\left(\frac{r}{a}\right)^{-2\mu/(1+\mu)}\right] \quad (11)$$

In this case, also, the mean stress was independent of the remote stress and increased away from the notch root.

The positions on the x-axis of the near-notch and far-notch boundaries of the stress-whitened zone are given in Table I for various remote stresses and three sample thicknesses. In all cases, the position of the near-notch boundary was constant at about 0.12 $\pm$ 0.03 mm from the notch tip, and because the plastic mean stress in the core yielding zone was independent of the remote stress and increased away from the notch surface, the value of σ_m calculated at the position of the near-notch boundary was the same in all cases. From Equation 11 a value of 43.0 $\pm$ 1.5 MPa was obtained. To illustrate the importance of the pressure dependence, this compared with a value of 48.6 MPa from Equation 7. The corresponding volume strain was calculated using values of 43.0 MPa for the mean stress, 3.7 GPa for the Young's modulus and 0.38 for Poisson's ratio of PVC. The value of 0.8 was the same as that obtained previously for blends of PVC, reinforcing the conclusion that the volume strain was a material property of PVC and the controlling parameter for cavitation.

The plastic–elastic stress distribution at a notch is amenable to finite element analysis, and the $\sigma_{\theta\theta}$–stress distribution available in the literature for a blunt notch was used to estimate the stress state at the far-notch boundary of the stress-whitened zone [21]. Because $\sigma_{\theta\theta}$ was the primary component of σ_m and determinations were confined to positions on the x-axis, comparison of $\sigma_{\theta\theta}$ values seemed a reasonable alternative to σ_m for evaluating the existence of a constant stress state at the far-notch boundary. Published $\sigma_{\theta\theta}$–stress distributions for steel [21] were normalized to the yield stress and $\sigma_{\theta\theta}$ obtained directly at the position of the far-notch boundary on the x-axis. The $\sigma_{\theta\theta}$ values, listed in Table I together with the position of the far-notch boundary, ranged from 61.1–78.3 MPa for the three sample thicknesses at various values of the remote stress. Although there was a rather large range in the stress values, the fact that there were no systematic trends with either sample thickness or remote stress suggested that the stress at the far-notch boundary was a constant. Furthermore, the values of $\sigma_{\theta\theta}$ at the far-notch boundary were very close to the value of 78.3 MPa for $\sigma_{\theta\theta}$ at the near-notch boundary obtained from the plastic analysis, Equations 8 and 9. Especially because an approximate method for a slightly different notch geometry was used to obtain the stress at the far-notch boundary, this was considered good evidence that the same stress condition was achieved at all points on the boundary of the stress-whitened zone regardless of whether it lay in the plastic zone or the elastic region.

TABLE I Near-notch and far-notch boundaries of the stress-whitened zone along the x-axis

Thickness (mm)	Remote stress (MPa)	Near-notch boundary (mm)	Far-notch boundary (mm)	Far-notch stress, $\sigma_{\theta\theta}$ (MPa)
1.6	35.5	1.14	1.40	74.9
	36.7	1.07	1.43	75.6
	38.4	1.10	1.62	78.3
	40.5	1.08	1.80	61.1
	41.6	1.08	1.85	61.1
3.6	34.0	1.11	1.43	66.6
	36.0	1.14	1.51	64.6
	38.6	1.13	1.64	61.8
	40.3	1.12	1.71	64.6
	41.1	1.12	1.81	61.1
4.9	35.2	1.14	1.35	74.9
	37.3	1.12	1.40	78.3
	38.8	1.14	1.53	71.4
	40.0	1.11	1.55	78.3
	41.4	1.14	1.59	71.4

The response of PVC when loaded in tension with a semicircular notch presented an intermediate situation between polycarbonate, for which only the shear modes were observed [9], and blends of PVC, where the cavitation mechanism dominated [10]. Assuming that whether the initial irreversible deformation occurred by a shear mode, specifically core yielding, or cavitation depended upon which stress condition was achieved first at the notch root, the remote stress required to achieve each critical condition was calculated for comparison. From the von Mises yield criterion, the remote stress required for core yielding in PVC was calculated to be 25.6 MPa using a value of 68.7 MPa for the yield stress in tension. This was considerably lower than 30.1 MPa, the remote stress calculated from the elastic stress distribution [10] that would have been required to initiate cavitation at the notch root. Once a plastic yielded zone formed, the resulting stress redistribution created a gradually increasing stress at the tip of the zone as it grew away from the notch root. In the case of PVC, the additional stress concentration was sufficient that the critical cavitational condition was achieved at the tip of the core yielded zone before the stress instability was reached.

3.5. Elastic stress redistribution

Growth of the damage zone after the stress-whitened zone initiated near the plastic zone tip occurred in such a way that the stress-whitened zone was located partially in the plastic zone and partly in the surrounding elastic region (cf. Fig. 2). The stress-whitened zone was used to estimate the redistribution of the elastic mean stress along the x-axis in the presence of

the core yielding zone. Assuming that the mean stress condition was achieved at all points on the boundary of the stress-whitened zone regardless of whether the zone lay in the plastic zone or the elastic region, the elastic mean stress at the far-notch boundary of the stress-whitened zone was the same as the plastic mean stress at the near-notch boundary, 43.0 MPa. Furthermore, the plastic mean stress and the elastic mean stress were equal and a maximum at the tip of the core yielding zone, so another point on the elastic mean stress curve could be calculated from Equation 11 if the location of the tip was known. This was discerned directly from the optical micrographs when the stress-whitened zone was small, otherwise the position of the tip of the core yielding zone was calculated from the width of the zone at the notch surface using Equation 3.

The plastic and elastic mean stress distributions along the x-axis were approximated for several values of the remote stress, Fig. 6. The plastic mean stress did not depend on the remote stress and was represented by a single curve emanating from the notch root. The two points at which the elastic mean stress was known, at the tip of the plastic yielded zone and at the far-notch boundary of the stress-whitened zone, were joined to approximate the elastic mean stress distribution outside the yielded zone. For comparison, the elastic mean stress distribution in the absence of a plastic zone was also plotted for the same values of the remote stress [10].

The results are qualitatively consistent with what is known about the effects of a plastic zone on elastic stress redistribution. Specifically, as the remote stress increased and the yielded zone increased in size, the so-called plastic stress concentration factor increased. This was somewhat analogous to the plastic zone acting as a notch because the material in the zone could not support stresses larger than the yield stress [22, 23]. The redistributed elastic stress became increasingly larger than the comparable elastic stress without the plastic zone, and the stress fell off more rapidly along the x-axis.

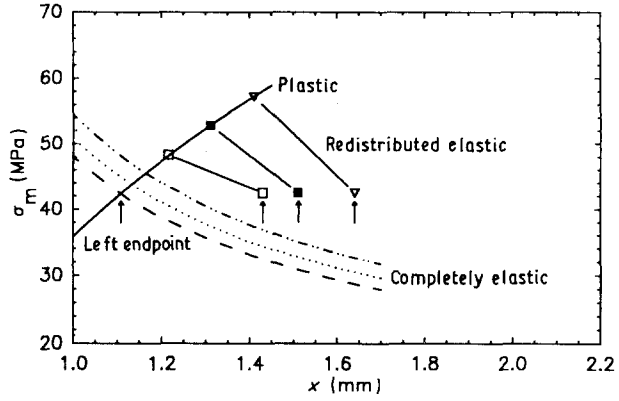

Figure 6 Approximated redistributed mean stress distribution along the x-axis for 3.6 mm thick PVC at several positions on the stress–displacement curve. The calculated elastic mean stress distribution [10] is included for comparison. (□ – –) 34.0 MPa, (■ · · ·) 36.0 MPa, (▽ – · · –) 38.6 MPa.

3.6. Stress instability

The thickness had no significant effect on the development of the damage zone up to position 4 on the stress–displacement curve. When viewed from the side, the core yielding zone and the stress-whitened zone had essentially the same appearance for the three thicknesses examined. The major effect of thickness was to increase the through-thickness dimension of the plane strain stress-whitened zone. The core yielding and stress-whitened zones were viewed by focusing on the centre of the specimen where these modes originated. The notch was photographed at higher stresses beginning with position 5 on the stress–displacement curve with the focus adjusted to the surface. Under these conditions, numerous surface crazes were visible, Fig. 7. The crazes, which followed the principal elastic stress contours [24], were caused by environmental effects because the craze density was greatly reduced when the surface was cleaned carefully.

At position 5 on the stress–displacement curve of the 3.6 mm thick sample (Fig. 7a, 46.5 MPa) two dark bands appeared above and below the stress-whitened zone. With increasing stress, position 6 (Fig. 7b, 50.2 MPa), these grew outward from the notch at an angle of approximately 40°. Near the maximum stress, position 7 (Fig. 7c, 52.8 MPa), the dark bands curved over and continued to elongate in a direction parallel to the x-axis until fracture occurred by ductile tearing through the damage zone. Two shear modes gave the damage zone its appearance in the 3.6 mm thick sheet [9]. Plane strain through-thickness yielding on inclined planes above and below the notch, referred to as hinge shear, was seen as the dark bands that first grew out at an angle from the notch surface. At higher stresses, plane stress intersecting shear occurred along planes parallel to the width direction.

Only the plane strain hinge shear mode was observed in thicker sheet. A 4.9 mm thick specimen loaded to 48.2 MPa, between the equivalent of positions 5 and 6 on the stress–displacement curve, showed only the hinge shear mode, Fig. 8a. Shown schematically in Fig. 8b, hinge shear occurred along planes normal to the plane of the sheet, so that the form was essentially the same at all interior sections, and at an angle to the notch that depended on the notch geometry. For PVC with a semicircular notch, this angle was about 40°, the same as polycarbonate [9].

The 4.6 mm thick specimen shown in Fig. 9a was loaded to 53.6 MPa, near the equivalent of position 7 on the stress–displacement curve, and sectioned in the yz plane through the damage zone. When the sectioned surface of this specimen was viewed end-on in the polarizing optical microscope, birefringent isostrain lines emanated from positions that corresponded with the ends of the dark hinge shear bands, Fig. 9b. The isostrain lines extended more or less horizontally through the thickness indicating that this mode of shear was through-thickness yielding. These micrographs also showed the size of the stress-whitened zone at higher stresses; although it had grown considerably in the x- and y-directions, it remained

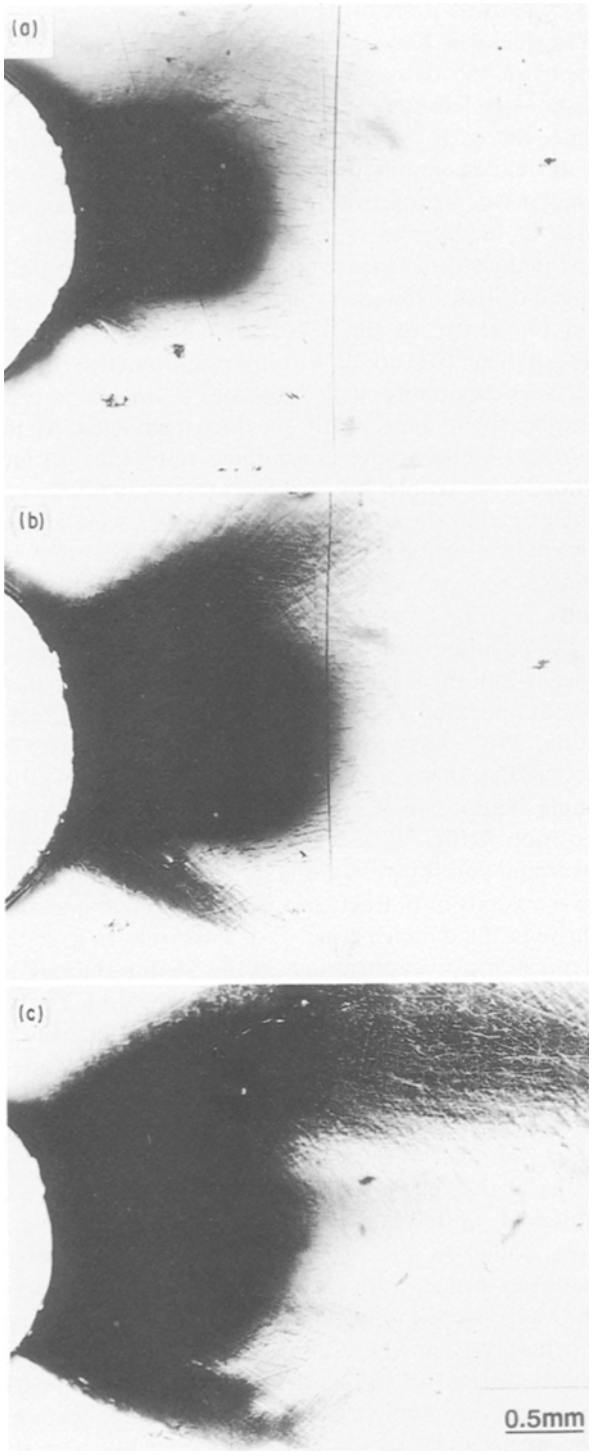

Figure 7 Optical micrographs of the damage zone of 3.6 mm thick PVC at higher stresses. (a) Position 5, 46.5 MPa, (b) position 6, 50.2 MPa, and (c) position 7, 52.8 MPa.

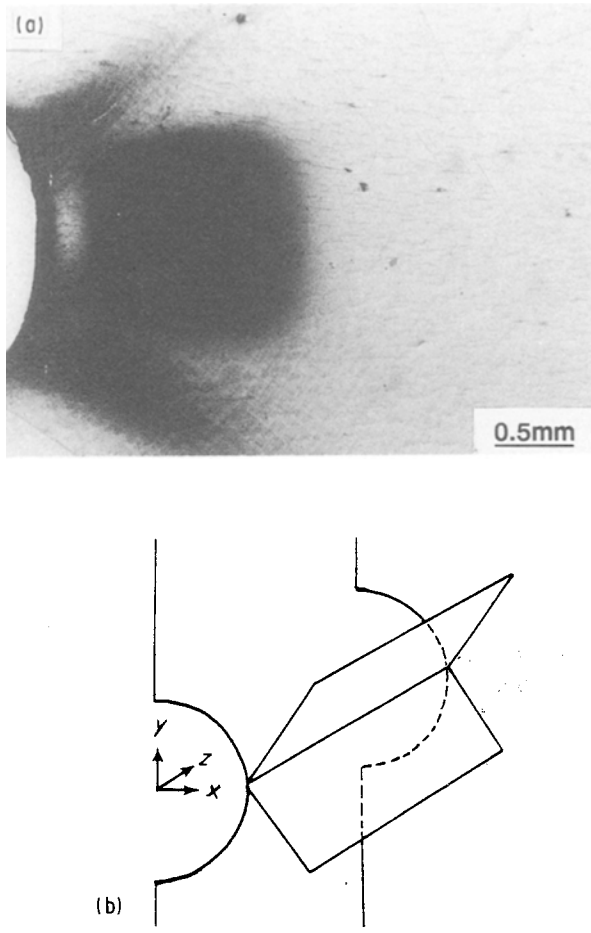

Figure 8 The hinge shear mode. (a) Optical micrograph of the damage zone of 4.9 mm thick PVC loaded to 48.2 MPa, and (b) schematic representation of hinge shear.

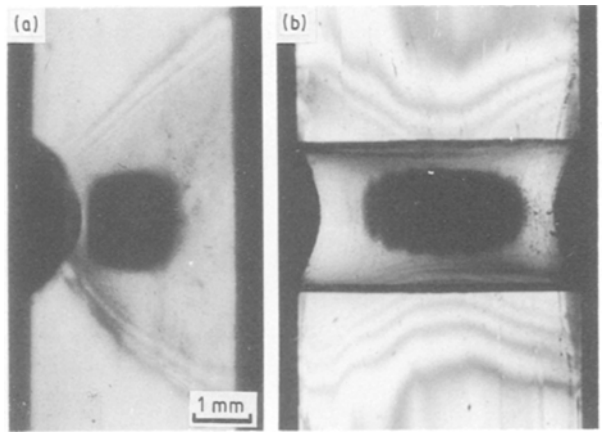

Figure 9 A 4.6 mm thick specimen loaded to 53.6 MPa and sectioned through the damage zone. (a) Side view of the sectioned specimen, and (b) the sectioned surface viewed end-on in the polarizing optical microscope.

confined to the plane strain region in the centre of the specimen.

The plane stress intersecting shear mode predominated in thinner sheet such as the 1.6 mm thick specimen loaded to 45.2 MPa shown in Fig. 10a. This shear mode, shown schematically in Fig. 10b, was projected in front of the notch and occurred along planes inclined at an angle to the tensile direction. The parallel bands of intersecting shear were closer together in the 1.6 mm thick sheet than in the 3.6 mm. Because the dark bands in the optical microscope occurred where the flow lines intersected the surface, the distance separating the parallel bands depended on the thickness of the sheet. For both thicknesses, the separation of the parallel bands was equal to t cot 53° where t was the thickness and 53° the angle at which the flow lines extended through the thickness. Close examination of the dark bands of hinge and intersecting shear showed that the flow planes contained numerous microshear bands. These bands were not observed with hinge or

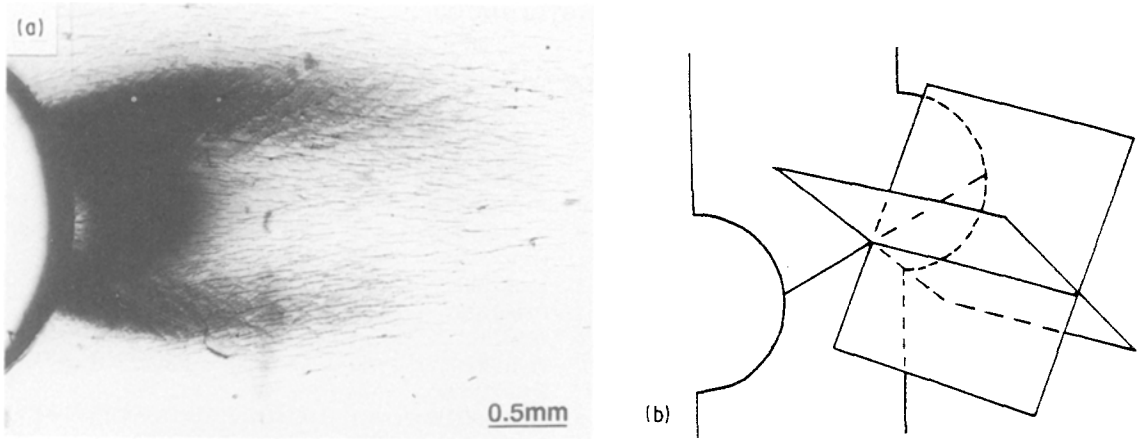

Figure 10 The intersecting shear mode. (a) Optical micrograph of the damage zone of 1.6 mm thick PVC loaded to 45.2 MPa, and (b) schematic representation of intersecting shear.

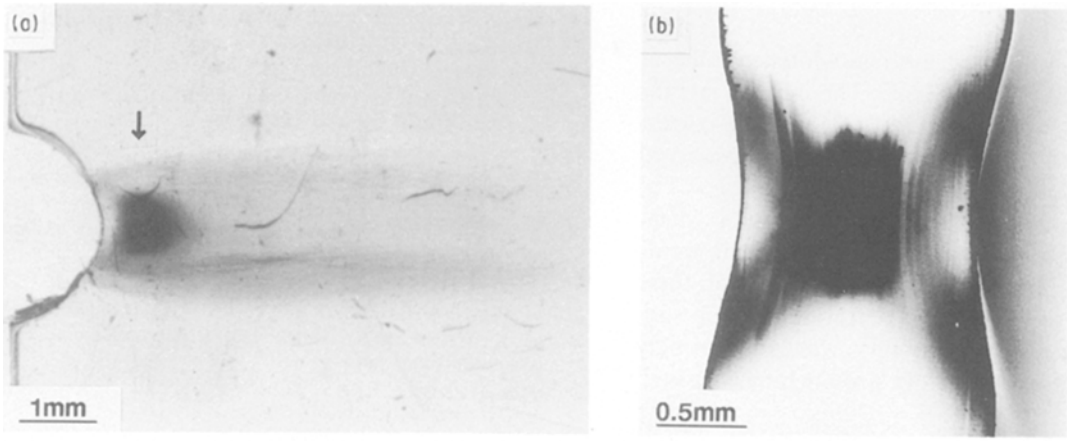

Figure 11 A. 1.6 mm thick specimen load to 51.3 MPa. (a) Side view, the arrow indicates the position of subsequent sectioning, and (b) the sectioned specimen viewed end-on in the polarizing optical microscope.

intersecting shear in polycarbonate [9], they were probably caused by local stress concentrations at the same heterogeneities in the PVC that were responsible for promoting stress whitening.

The intersecting shear planes lengthened out from the notch at higher stresses as more of the specimen width reached the yield stress. A damage zone that had progressed some distance across the width, Fig. 11a, was sectioned at the location of the arrow. The section, at a higher magnification in Fig. 11b, showed, superimposed on the stress-whitened zone, the flow lines of intersecting shear that extended through the thickness at an angle to the loading direction. The micrograph also showed the necking effect produced by intersecting shear. To accommodate the strain at the notch tip, the shear planes broadened so that the region between the planes became progressively thinner.

Only the 3.6 mm thick sheet clearly exhibited the transition from hinge shear to intersecting shear that was previously reported in polycarbonate [9]; the dominant shear mode in the thinner sheet was intersecting shear and in the thicker sheet was hinge shear. The onset stresses of hinge shear and intersecting shear were obtained from the series of micrographs which accompanied tensile loading of the three thicknesses of PVC, although particularly for the thickest sheet the beginning of hinge shear was obscured by the stress-whitened zone and the onset stress was difficult to determine accurately. The conditions under which plane strain hinge shear and plane stress intersecting shear should be dominant [25] have been confirmed for polycarbonate [9]. For purposes of comparison with polycarbonate, the onset stresses for PVC were determined as a percentage of the yield stress using the same conditions as employed previously. Intersecting shear was observed at 71% of the yield stress for 1.6 mm thick PVC compared to 74% for 1.20 mm thick PC; hinge shear and intersecting shear were observed at 79% and 86%, respectively, for 3.6 mm thick PVC compared to 69% and 89% for 3.14 mm thick PC; and hinge shear was observed at 76% of the yield stress for 4.9 mm thick PVC compared with 73% for 4.70 mm thick PC.

The observation that hinge and intersecting shear in PVC closely conformed with the characteristics established for polycarbonate, a material that deformed only by shear under these conditions, suggested that the shear yielding modes were superimposed on the cavitation mechanism in PVC with little or no effect of

the stress-whitened zone. This was in contrast to the blends of PVC where growth of the stress-whitened zone relieved the through-thickness constraint so that the plane strain hinge shear mode was not observed in thick sheet. The difference was attributed to the confined nature of the stress-whitened zone in PVC and the fact that, unlike the blends, the stress-whitened zone did not extend to the notch surface where it could have had a significant notch-blunting effect.

4. Conclusions

Analysis of the damage zone that formed ahead of a semicircular notch in PVC sheet during slow tensile loading led to the following conclusions.

1. Core yielding was observed at the notch root. The two families of intersecting slip lines were similar to those observed in polycarbonate and were described by plasticity analysis of a pressure-dependent material.

2. Cavitation produced a stress-whitened zone at the tip of the core yielding zone. The mean stress for cavitation was found to be 43.0 MPa and the corresponding volume strain was the same as observed previously in blends of PVC.

3. At higher stresses, the plane strain hinge shear mode and the plane stress intersecting shear mode were observed. The thickness dependence of these modes was the same as in polycarbonate which suggested that the stress instability was not strongly affected by the presence of the stress-whitened zone.

Acknowledgements

The authors thank Professor A. S. Argon for his helpful comments, and Dr Ray Laakso, The Dow Chemical Company, Plaquemine, LA, for providing the poly(vinyl chloride). This research was generously supported by The National Science Foundation, Polymers Program (DMR 87-13041).

References

1. K. V. GOTHAM, *Plastics Polymers* **37** (1969) 309.
2. P. I. VINCENT, F. M. WILLMOUTH and A. J. COBBOLD, in Preprints "2nd International Conference on Yield, Deformation and Fracture of Polymers", Cambridge, UK (The Plastics Institute, 1973) p. 5/1.
3. P. L. CORNES and R. N. HAWARD, *Polymer* **15** (1974) 149.
4. A. SIEGMANN, L. K. ENGLISH, E. BAER and A. HILTNER, *Polym. Engng Sci* **24** (1984) 877.
5. L. H. LEE, J. F. MANDELL and F. J. McGARRY, *ibid.* **26** (1986) 626.
6. *Idem, ibid.* **27** (1987) 1128.
7. H. BERGKVIST and H. ANDERSSON, *Int. J. Fract. Mech.* **8** (1972) 139.
8. H. R. BROWN and T. H. CHIN, *J. Mater. Sci.* **15** (1980) 677.
9. M. MA, K. VIJAYAN, J. IM, A. HILTNER and E. BAER, *ibid.* **24** (1989) 2687.
10. A. TSE, E. SHIN, R. LAAKSO, A. HILTNER and E. BAER, *ibid.* **26** (1991) 2823.
11. M. KITAGAWA, *ibid.* **17** (1982) 2514.
12. I. NARISAWA, M. ISHIKAWA and H. OGAWA, *ibid.* **15** (1980) 2059.
13. M. ISHIKAWA, H. OGAWA and I. NARISAWA, *J. Macromol. Sci. Phys.* **B19** (1981) 421.
14. N. J. MILLS, *J. Mater. Sci.* **11** (1976) 363.
15. I. NARISAWA, M. ISHIKAWA and H. OGAWA, *J. Polym. Sci. Polym. Phys. Ed.* **15** (1977) 2227.
16. S. N. ZHURKOV, *Int. J. Fract.* **11** (1975) 629.
17. J. F. KNOTT and A. H. COTTRELL, *J. Iron Steel Inst.* **201** (1963) 249.
18. R. HILL, "The Mathematical Theory of Plasticity" (Clarendon, Oxford, 1950).
19. P. B. BOWDEN and J. A. JUKES, *J. Mater. Sci.* **7** (1972) 52.
20. J. YUAN, A. HILTNER and E. BAER, *ibid.* **18** (1983) 3063.
21. K. KUEHNE, J. REDMER and W. DAHL, *Engng Fract. Mech.* **16** (1982) 845.
22. J. A. HENDRICKSON, D. S. WOOD and D. S. CLARK, *Trans. ASM* **50** (1958) 656.
23. T. R. WILSHAW, C. A. RAU and A. S. TETELMAN, *Engng Fract. Mech.* **1** (1968) 191.
24. M. BEVIS and D. HULL, *J. Mater. Sci.* **5** (1970) 293.
25. G. T. HAHN and A. R. ROSENFIELD, *Acta Metall.* **13** (1965) 293.

Received 16 October 1990
and accepted 9 January 1991